Few-body reference data for multicomponent formalisms: Light-nuclei molecules

Ilkka Kylänpää,[1] Tapio T. Rantala,[2] and David M. Ceperley[1]
[1]*Department of Physics, University of Illinois at Urbana-Champaign, Illinois 61801, USA*
[2]*Department of Physics, Tampere University of Technology, P.O. Box 692, FI-33101 Tampere, Finland*
(Received 14 August 2012; revised manuscript received 2 October 2012; published 14 November 2012)

We present full quantum statistical energetics of some electron–light-nuclei systems. This is accomplished with the path-integral Monte Carlo method. The effects on energetics arising from the change in the nuclear mass are studied. The obtained results may serve as reference data for the multicomponent density functional theory calculations of light-nuclei systems. In addition, the results reported here will enable better fitting of today's electron-nuclear energy functionals, for which the description of light nuclei is most challenging in particular.

DOI: 10.1103/PhysRevA.86.052506 PACS number(s): 31.15.A−, 31.15.E−

Density functional theory (DFT) is among the most successful approaches to calculate the electronic structure of atoms, molecules, and solids. A similar approach, however, including more degrees of freedom was introduced in 2001 by Kreibich and Gross [1] and is called the multicomponent density functional theory (MCDFT). In contrast to the original form of the DFT, MCDFT enables the complete quantum treatment of many-particle systems consisting of electrons and nuclei. As is well known, the original form of DFT incorporates the Born-Oppenheimer approximation for the nuclei [2,3].

With the MCDFT approach, it is possible to extend the success of DFT into an entirely new field of applications, such as the first-principles calculation of electron-phonon coupling in solids [4,5], polaronic motion [6], and positron scattering and annihilation [7–9]. That is, with MCDFT, physical phenomena that depend on a strong coupling between electronic and nuclear motion can be evaluated from first principles.

The original DFT is also known for its need for good functional forms, especially for the exchange and correlation functionals. One of the most widely employed functionals is the so-called local density approximation (LDA), which uses the Monte Carlo data of the free electron gas [10] as a basic input. Proper functional forms are also needed in the MCDFT scheme, for the electron-nuclear energy functional [11,12] in particular. For the present, the absence of good multicomponent reference data is slowing down the development of new functional forms for the MCDFT. The main difficulties are encountered in the description of light nuclei.

In this paper, we will provide few-body reference data for light-nuclei systems, which can be used in the development of better MCDFT functionals and improvement of the present fits. This is accomplished with full quantum statistical simulations using the path-integral Monte Carlo (PIMC) approach [13], which is a basis-function-independent and trial-wave-function-independent approach including many-body correlations exactly. The nuclear mass is given values ranging from that of a positron to that of a proton described by the following systems: $x^+e_2{}^-$, $x_2{}^+e^-$, $x^+p^+e^-$, $x_2{}^+e_2{}^-$, $x^+p^+e_2{}^-$, and $x^+e^+e_2{}^-$, where x^+ goes from positron (e^+) to proton (p^+). A more detailed description of our approach is given in Ref. [14].

According to the Feynman formulation of the quantum statistical mechanics [15], the partition function for interacting distinguishable particles is given by the trace of the density matrix:

$$Z = \mathrm{Tr}\hat{\rho}(\beta) = \int dR_0 dR_1 \ldots dR_{M-1} \prod_{i=0}^{M-1} e^{-S(R_i,R_{i+1};\tau)},$$

where $\hat{\rho}(\beta) = e^{-\beta\hat{H}}$, S is the action, $\beta = 1/k_BT$, $\tau = \beta/M$, $R_M = R_0$, and M is called the Trotter number. In this paper, we use the pair approximation in the action [13,16] for the Coulomb interaction of charges. Sampling in the configuration space is carried out using the Metropolis procedure [17] with multilevel bisection moves [18]. The total energy is calculated using the virial estimator [19].

In the following, we use atomic units, where the lengths, energies, and masses are given in units of the Bohr radius (a_0), hartree (E_h), and free electron mass (m_e), respectively. The statistical standard error of the mean with 2σ limits is used as an error estimate for the observables. However, in the case of the contact densities, the error estimates also include a contribution resulting from extrapolation to origin.

In our model, all of the particles are described as "Boltzmannons," i.e., they obey the Boltzmann statistics. For the present study, the particles involved can be treated accurately as distinguishable particles. This is possible by assigning spin-up to one electron and spin-down to the other one, and applying the same for the positive particles. This is accurate enough, as long as the thermal energy is well below that of the lowest electronic triplet excitation, ΔE_{st}. For the systems under consideration, $\Delta E_{st} > 0.18E_\mathrm{h}$, with the smallest being that of the Ps_2 molecule [20,21]. For systems consisting of distinguishable particles, the accuracy of the PIMC method is determined by the imaginary-time "time step" τ only. As τ approaches zero, the exact many-body results are obtained. For more details on our model, see Ref. [14].

In the simulations, we use $m_e = 1 = m_{e^+}$ as the mass of the electrons and the positron, and, for the protons, we use $m_p = 1836.1527m_e$. The simulations are carried out at 300 K temperature, and for the Trotter number, we have chosen $M = 8192$. This leads to imaginary-time time step $\tau = \beta/M \approx 0.1285E_\mathrm{h}^{-1}$, which ensures good-enough accuracy in the case of light nuclei—the error is of the order of $O(\tau^3)$. The simulations apply the minimum image convention and a cubic simulation cell, $V = (300a_0)^3$.

In Figs. 1 and 2, we show the total energy as a function of mass of the nuclei, i.e., the positive particles: On the left,

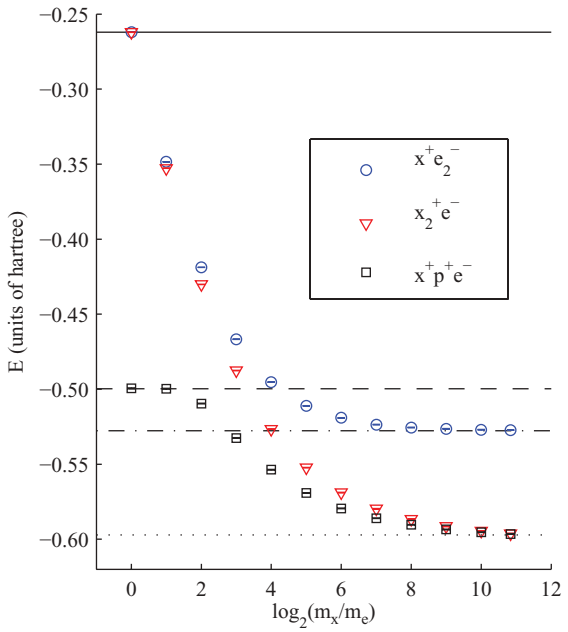

FIG. 1. (Color online) Total energy as a function of mass of the nuclei, i.e., positive particles. Blue circles show the energy of $x^+e_2^-$, red down-triangles show that of $x_2^+e^-$, and black squares show that of $x^+p^+e^-$, where x^+ goes from e^+ to p^+. The reference energies are given as solid, dashed, dash-dotted, and dotted lines corresponding to Ps^- (as well as Ps_2^+), ^1H, $^1H^-$, and $^1H_2^+$, respectively.

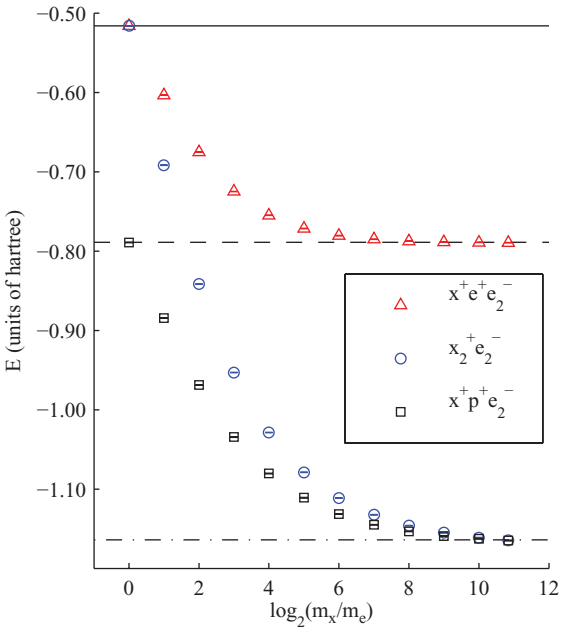

FIG. 2. (Color online) Total energy as a function of mass of the nuclei, i.e., positive particles. Red up-triangles show the energy of $x^+e^+e_2^-$, blue circles show that of $x_2^+e_2^-$, and black squares show that of $x^+p^+e_2^-$, where x^+ goes from e^+ to p^+. The reference energies are given as solid, dashed, and dash-dotted lines corresponding to Ps_2, ^1HPs, and $^1H_2$, respectively.

TABLE I. Total energies at different nuclear masses; see also Figs. 1 and 2. Energies are given in units of hartree with 2σ error estimates. Reading from top to bottom, the x^+ in the table goes from positron to proton—the mass of the particle increases.

$\log_2(m_x/m_e)$	$x^+e_2^-$	$x_2^+e^-$	$x^+p^+e^-$	$x_2^+e_2^-$	$x^+e^+e_2^-$	$x^+p^+e_2^-$
0.0000	−0.26205(8)	−0.26212(8)	−0.4994(4)	−0.5162(2)	−0.5162(2)	−0.7892(3)
1.0000	−0.34850(10)	−0.35278(10)	−0.4997(4)	−0.6917(3)	−0.6034(2)	−0.8844(3)
2.0000	−0.41876(12)	−0.43018(13)	−0.5096(2)	−0.8417(3)	−0.6751(2)	−0.9688(4)
3.0000	−0.46670(13)	−0.48760(15)	−0.5325(2)	−0.9531(3)	−0.7249(2)	−1.0344(4)
4.0000	−0.49530(15)	−0.5267(2)	−0.5536(2)	−1.0288(3)	−0.7550(2)	−1.0804(4)
5.0000	−0.5111(2)	−0.5522(2)	−0.5692(2)	−1.0788(3)	−0.7715(3)	−1.1109(4)
6.0000	−0.5192(2)	−0.5689(2)	−0.5795(2)	−1.1112(3)	−0.7806(3)	−1.1316(4)
7.0000	−0.5236(2)	−0.5797(2)	−0.5860(2)	−1.1324(3)	−0.7851(3)	−1.1450(4)
8.0000	−0.5256(2)	−0.5866(2)	−0.5903(2)	−1.1462(3)	−0.7874(3)	−1.1534(3)
9.0000	−0.5265(3)	−0.5914(2)	−0.5935(2)	−1.1550(4)	−0.7886(3)	−1.1591(4)
10.0000	−0.5271(2)	−0.5945(2)	−0.5953(2)	−1.1611(4)	−0.7891(3)	−1.1626(4)
10.8425	−0.5273(3)	−0.5962(2)	−0.5965(3)	−1.1648(4)	−0.7894(3)	−1.1648(4)

TABLE II. Comparison of the PIMC and reference total energies. Absolute value of the difference in energies $|\Delta E|$ is also given. Energies are given in units of hartree with 2σ error estimates.

	Ps^-	$^1H^-$	$^1H_2^+$	Ps_2	^1HPs	$^1H_2$
PIMC	−0.2620857(679)	−0.527262(201)	−0.596350(167)	−0.516218(121)	−0.789274(125)	−1.164830(224)
Refs.	−0.262005070233[a]	−0.527445881114[b]	−0.5971390625[c]	−0.516003790416[d]	−0.788870710444[d]	−1.16402503063[e]
$\|\Delta E\|$	0.000081	0.000184	0.000790	0.000215	0.000404	0.000805

[a]Drake *et al.* [24].
[b]Frolov [25].
[c]Bishop *et al.* [26].
[d]Bubin and Adamowicz [27].
[e]Stanke *et al.* [28].

TABLE III. Direct comparison of energetics to (a) Mitroy and Novikov (2004) [22] and to (b) Bromley and Mitroy (2002) [23] for the case $x^+e^+e_2^-$. Absolute value of the difference in energies $|\Delta E|$ is also given. Energies are given in units of hartree with 2σ error estimates.

m_x/m_e	PIMC	Refs.	$\lvert\Delta E\rvert$
1.314	−0.551563(171)	−0.54952[b]	0.002043
0.656	−0.462815(138)	−0.460456[a]	0.002359
0.607	−0.453311(126)	−0.446810[a]	0.006501
0.600	−0.451962(129)	−0.451931[a]	0.000031
0.469	−0.423690(120)	−0.414066[a]	0.009624
0.100	−0.308262(102)	−0.307961[a]	0.000301
0.020	−0.271874(169)	−0.271875[a]	0.000001

TABLE IV. Expectation values at different nuclear masses for $x_2{}^+e^-$: total energy, interparticle distances and their second moments as well as their first inverse moments, and contact densities. Values are given in atomic units, and a 2σ error estimate is shown in the parentheses. For the contact densities, the error estimates also include a contribution resulting from extrapolation to origin. Reading from left to right, the x^+ in the table goes from positron to proton—the mass of the particle increases.

$\log_2$ (m_x/m_e)	0.0000	1.0000	2.0000	3.0000	4.0000	5.0000	6.0000	7.0000	8.0000	9.0000	10.0000	10.8425
E	−0.26212(8)	−0.3528(1)	−0.4302(2)	−0.4876(2)	−0.5267(2)	−0.5522(2)	−0.5689(2)	−0.5797(2)	−0.5866(2)	−0.5914(2)	−0.5945(2)	−0.5962(2)
$\langle r_{e^-x^+}\rangle$	5.466(9)	3.833(6)	2.941(3)	2.439(3)	2.151(2)	1.979(2)	1.872(2)	1.8037(9)	1.7598(9)	1.7297(8)	1.7097(8)	1.6981(8)
$\langle r_{x^+x^+}\rangle$	8.50(2)	5.77(2)	4.257(6)	3.393(4)	2.889(3)	2.584(2)	2.392(2)	2.269(2)	2.188(2)	2.133(2)	2.095(2)	2.074(2)
$\langle r^2_{e^-x^+}\rangle$	47.8(3)	22.3(2)	12.45(4)	8.17(2)	6.14(1)	5.084(7)	4.481(6)	4.116(5)	3.888(4)	3.737(4)	3.638(4)	3.581(4)
$\langle r^2_{x^+x^+}\rangle$	92.0(5)	40.9(3)	21.50(7)	13.17(4)	9.26(2)	7.22(2)	6.072(9)	5.376(8)	4.942(7)	4.655(6)	4.464(6)	4.355(6)
$\langle r^{-1}_{e^-x^+}\rangle$	0.3402(2)	0.4634(2)	0.5736(3)	0.6598(3)	0.7213(4)	0.7633(4)	0.7916(4)	0.8105(4)	0.8228(4)	0.8314(4)	0.8371(4)	0.8404(4)
$\langle r^{-1}_{x^+x^+}\rangle$	0.1562(2)	0.2213(3)	0.2869(3)	0.3444(4)	0.3893(4)	0.4221(3)	0.4454(3)	0.4616(3)	0.4724(3)	0.4800(3)	0.4854(3)	0.4884(3)
$\langle\delta(r_{e^-x^+})\rangle$	0.0202(8)	0.049(3)	0.087(4)	0.124(7)	0.152(8)	0.171(9)	0.18(1)	0.19(1)	0.19(2)	0.20(2)	0.20(2)	0.20(2)
$\langle\delta(r_{x^+x^+})\rangle$	0.000065(6)	0.00011(2)	0.00009(2)	0.000029(9)	0.000003(2)	0.00000003(7)	0.00(0)	0.00(0)	0.00(0)	0.00(0)	0.00(0)	0.00(0)

TABLE V. Expectation values at different nuclear masses for $x_2{}^+e_2^-$: total energy, interparticle distances and their second moments as well as their first inverse moments, and contact densities. Values are given in atomic units, and a 2σ error estimate is shown in the parentheses. For the contact densities, the error estimates also include a contribution resulting from extrapolation to origin. Reading from left to right, the x^+ in the table goes from positron to proton—the mass of the particle increases.

$\log_2$ (m_x/m_e)	0.0000	1.0000	2.0000	3.0000	4.0000	5.0000	6.0000	7.0000	8.0000	9.0000	10.0000	10.8425
E	−0.5162(2)	−0.6917(3)	−0.8417(3)	−0.9531(3)	−1.0288(3)	−1.0788(3)	−1.1112(3)	−1.1324(3)	−1.1462(3)	−1.1550(4)	−1.1611(4)	−1.1648(4)
$\langle r_{e^-e^-}\rangle$	6.01(4)	4.44(2)	3.467(7)	2.929(3)	2.635(2)	2.465(2)	2.362(1)	2.2976(9)	2.2562(8)	2.2294(8)	2.2113(8)	2.2001(8)
$\langle r_{e^-x^+}\rangle$	4.47(2)	3.25(1)	2.533(4)	2.135(2)	1.913(2)	1.7829(8)	1.7030(7)	1.6520(6)	1.6192(6)	1.5979(6)	1.5834(6)	1.5744(5)
$\langle r_{x^+x^+}\rangle$	6.01(4)	4.18(2)	3.043(8)	2.403(4)	2.038(2)	1.819(2)	1.681(1)	1.5905(9)	1.5316(8)	1.4929(8)	1.4660(7)	1.4495(7)
$\langle r^2_{e^-e^-}\rangle$	45.9(8)	24.8(3)	14.74(8)	10.38(3)	8.36(2)	7.302(8)	6.699(6)	6.333(5)	6.103(5)	5.957(5)	5.859(5)	5.799(4)
$\langle r^2_{e^-x^+}\rangle$	28.8(4)	14.9(2)	8.70(4)	6.01(2)	4.749(7)	4.089(4)	3.711(3)	3.481(3)	3.336(3)	3.243(3)	3.181(3)	3.144(3)
$\langle r^2_{x^+x^+}\rangle$	45.9(8)	21.8(3)	11.10(8)	6.65(3)	4.63(1)	3.595(5)	3.006(4)	2.649(3)	2.426(3)	2.284(3)	2.187(2)	2.129(2)
$\langle r^{-1}_{e^-e^-}\rangle$	0.2214(7)	0.2982(8)	0.3763(5)	0.4407(4)	0.4872(3)	0.5192(3)	0.5408(3)	0.5554(3)	0.5650(2)	0.5713(3)	0.5757(2)	0.5784(2)
$\langle r^{-1}_{e^-x^+}\rangle$	0.3688(5)	0.4979(5)	0.6164(4)	0.7094(4)	0.7752(4)	0.8200(3)	0.8500(3)	0.8701(3)	0.8834(3)	0.8921(3)	0.8981(3)	0.9019(3)
$\langle r^{-1}_{x^+x^+}\rangle$	0.2214(7)	0.3101(8)	0.4060(6)	0.4906(5)	0.5558(5)	0.6031(4)	0.6368(4)	0.6605(4)	0.6765(4)	0.6870(4)	0.6946(4)	0.6993(4)
$\langle\delta(r_{e^-e^-})\rangle$	0.00022(2)	0.00069(5)	0.00140(8)	0.0025(2)	0.0036(2)	0.0043(2)	0.0048(2)	0.0052(3)	0.0053(3)	0.0055(3)	0.0056(3)	0.0057(3)
$\langle\delta(r_{e^-x^+})\rangle$	0.0219(8)	0.053(3)	0.093(5)	0.132(7)	0.163(9)	0.18(1)	0.20(2)	0.21(2)	0.21(2)	0.22(2)	0.22(2)	0.22(2)
$\langle\delta(r_{x^+x^+})\rangle$	0.00023(2)	0.00046(5)	0.00046(7)	0.00022(6)	0.00004(2)	0.000002(3)	0.00(0)	0.00(0)	0.00(0)	0.00(0)	0.00(0)	0.00(0)

TABLE VI. Expectation values at different nuclear masses for $x^+p^+e_2^-$: total energy, interparticle distances and their second moments as well as their first inverse moments, and contact densities. Values are given in atomic units, and a 2σ error estimate is shown in the parentheses. For the contact densities, the error estimates also include a contribution resulting from extrapolation to origin. Reading from left to right, the x^+ in the table goes from positron to proton—the mass of the particle increases.

$\log_2(m_x/m_e)$	0.0000	1.0000	2.0000	3.0000	4.0000	5.0000	6.0000	7.0000	8.0000	9.0000	10.0000	10.8425
E	−0.7892(3)	−0.8843(3)	−0.9688(4)	−1.0344(4)	−1.0804(4)	−1.1109(4)	−1.1316(4)	−1.1450(4)	−1.1534(4)	−1.1591(4)	−1.1626(4)	−1.1648(4)
$\langle r_{e^-e^-}\rangle$	3.574(7)	3.176(5)	2.845(4)	2.610(2)	2.458(2)	2.363(2)	2.2998(9)	2.2597(9)	2.2341(8)	2.2173(8)	2.2065(8)	2.2003(8)
$\langle r_{e^-x^+}\rangle$	3.480(4)	2.693(3)	2.239(2)	1.971(2)	1.8139(9)	1.7204(7)	1.6621(7)	1.6260(6)	1.6033(6)	1.5888(6)	1.5797(6)	1.5746(6)
$\langle r_{e^-p^+}\rangle$	2.312(4)	2.120(3)	1.955(2)	1.830(2)	1.7446(9)	1.6867(8)	1.6457(7)	1.6180(7)	1.5999(6)	1.5875(6)	1.5794(6)	1.5745(6)
$\langle r_{x^+p^+}\rangle$	3.661(7)	2.854(5)	2.346(4)	2.019(3)	1.813(2)	1.682(2)	1.594(1)	1.5366(9)	1.4992(8)	1.4746(7)	1.4588(7)	1.4493(7)
$\langle r^2_{e^-e^-}\rangle$	15.89(8)	12.33(5)	9.79(3)	8.20(2)	7.261(9)	6.701(6)	6.345(5)	6.122(5)	5.982(5)	5.891(5)	5.833(4)	5.800(4)
$\langle r^2_{e^-x^+}\rangle$	15.59(4)	9.38(3)	6.47(2)	4.999(7)	4.217(5)	3.782(4)	3.521(3)	3.364(3)	3.266(3)	3.204(3)	3.166(3)	3.144(3)
$\langle r^2_{e^-p^+}\rangle$	7.82(4)	6.24(3)	5.11(2)	4.378(7)	3.927(5)	3.646(4)	3.456(3)	3.332(3)	3.253(3)	3.199(3)	3.164(3)	3.144(3)
$\langle r^2_{x^+p^+}\rangle$	16.26(8)	9.64(5)	6.31(3)	4.54(2)	3.571(7)	3.010(5)	2.662(4)	2.445(3)	2.307(3)	2.218(3)	2.162(2)	2.129(2)
$\langle r^{-1}_{e^-e^-}\rangle$	0.3705(4)	0.4109(4)	0.4540(4)	0.4920(4)	0.5207(3)	0.5408(3)	0.5548(3)	0.5641(3)	0.5702(2)	0.5742(2)	0.5768(2)	0.5784(3)
$\langle r^{-1}_{e^-x^+}\rangle$	0.4187(2)	0.5469(3)	0.6583(4)	0.7433(4)	0.8017(4)	0.8395(4)	0.8643(3)	0.8798(3)	0.8895(3)	0.8957(3)	0.8995(3)	0.9019(3)
$\langle r^{-1}_{e^-p^+}\rangle$	0.7295(4)	0.7573(5)	0.7879(5)	0.8172(4)	0.8415(4)	0.8601(4)	0.8744(4)	0.8848(4)	0.8916(3)	0.8966(3)	0.8998(3)	0.9018(3)
$\langle r^{-1}_{x^+p^+}\rangle$	0.3476(4)	0.4289(5)	0.5007(6)	0.5600(5)	0.6047(5)	0.6366(5)	0.6595(4)	0.6750(4)	0.6853(4)	0.6921(4)	0.6966(4)	0.6994(4)
$\langle\delta(r_{e^-e^-})\rangle$	0.00149(9)	0.0019(1)	0.0030(2)	0.0037(2)	0.0044(2)	0.0049(3)	0.0051(3)	0.0053(3)	0.0055(3)	0.0056(3)	0.0057(3)	0.0057(3)
$\langle\delta(r_{e^-x^+})\rangle$	0.0243(9)	0.057(3)	0.099(5)	0.139(7)	0.170(9)	0.19(1)	0.20(2)	0.21(2)	0.21(2)	0.22(2)	0.22(2)	0.22(2)
$\langle\delta(r_{e^-p^+})\rangle$	0.173(9)	0.18(1)	0.19(1)	0.19(2)	0.20(2)	0.21(2)	0.21(2)	0.21(2)	0.22(2)	0.22(2)	0.22(2)	0.22(2)
$\langle\delta(r_{x^+p^+})\rangle$	0.00028(3)	0.00024(3)	0.00011(3)	0.00002(1)	0.000001(2)	0.00000000(3)	0.00(0)	0.00(0)	0.00(0)	0.00(0)	0.00(0)	0.00(0)

x^+ is equal to a positron; on the right, x^+ corresponds to a proton; and in the middle region, we assign ten different masses for the x^+ particle.

The total energies are also given in Table I. The time-step error affects mainly the fourth decimal in the total energies, which can be validated by comparing the end-point values in Table I to high-accuracy zero Kelvin results; see Table II for more details. The comparison shows that the difference between high-accuracy results and our PIMC values is less than $0.00081E_h^{-1}$, which also confirms that the order of the time-step error is $O(\tau^3)$. Since the fourth decimal is also uncertain due to statistical error estimate, the present time-step error is considered acceptable. All energies given in Table I are from separate long-enough simulations, and a number of other observables, such as interparticle distances and contact densities, are presented in Tables IV–VIII.

TABLE VII. Expectation values at different nuclear masses for $x^+e^+e_2^-$: total energy, interparticle distances and their second moments as well as their first inverse moments, and contact densities. Values are given in atomic units, and a 2σ error estimate is shown in the parentheses. For the contact densities, the error estimates also include a contribution resulting from extrapolation to origin. Reading from left to right, the x^+ in the table goes from positron to proton—the mass of the particle increases.

$\log_2(m_x/m_e)$	0.0000	1.0000	2.0000	3.0000	4.0000	5.0000	6.0000	7.0000	8.0000	9.0000	10.0000	10.8425
E	−0.5162(2)	−0.6034(2)	−0.6751(2)	−0.7249(2)	−0.7550(2)	−0.7715(3)	−0.7806(3)	−0.7851(3)	−0.7874(3)	−0.7886(3)	−0.7891(3)	−0.7894(3)
$\langle r_{e^-e^-}\rangle$	6.00(4)	5.12(4)	4.48(3)	4.05(2)	3.814(9)	3.700(8)	3.626(7)	3.598(7)	3.581(7)	3.570(7)	3.572(7)	3.569(7)
$\langle r_{e^-e^+}\rangle$	4.47(2)	4.11(2)	3.85(2)	3.673(7)	3.576(5)	3.530(4)	3.500(4)	3.489(4)	3.482(3)	3.477(3)	3.478(4)	3.477(4)
$\langle r_{e^-x^+}\rangle$	4.47(2)	3.55(2)	3.00(2)	2.668(7)	2.490(5)	2.404(5)	2.351(4)	2.330(4)	2.318(4)	2.310(4)	2.311(4)	2.309(4)
$\langle r_{e^+x^+}\rangle$	6.00(4)	5.06(4)	4.46(3)	4.07(2)	3.864(9)	3.767(8)	3.704(7)	3.681(7)	3.666(6)	3.656(6)	3.659(7)	3.657(7)
$\langle r^2_{e^-e^-}\rangle$	45.7(8)	33.3(8)	25.5(5)	20.6(2)	18.1(2)	17.1(1)	16.33(9)	16.10(8)	15.93(8)	15.81(8)	15.85(8)	15.83(8)
$\langle r^2_{e^-e^+}\rangle$	28.8(4)	23.3(4)	19.9(3)	17.7(1)	16.60(6)	16.11(5)	15.79(5)	15.68(4)	15.60(4)	15.54(4)	15.56(4)	15.56(4)
$\langle r^2_{e^-x^+}\rangle$	28.8(4)	18.8(4)	13.5(3)	10.6(1)	9.14(6)	8.50(5)	8.09(5)	7.95(5)	7.85(4)	7.79(4)	7.80(4)	7.79(5)
$\langle r^2_{e^+x^+}\rangle$	45.7(8)	32.3(8)	24.9(5)	20.4(2)	18.2(2)	17.28(9)	16.65(8)	16.44(8)	16.29(7)	16.19(7)	16.23(8)	16.21(8)
$\langle r^{-1}_{e^-e^-}\rangle$	0.2215(7)	0.2603(9)	0.2979(9)	0.3282(6)	0.3477(5)	0.3583(5)	0.3650(5)	0.3679(5)	0.3695(5)	0.3705(4)	0.3705(5)	0.3708(5)
$\langle r^{-1}_{e^-e^+}\rangle$	0.3688(4)	0.3831(5)	0.3957(5)	0.4057(3)	0.4118(3)	0.4150(3)	0.4171(3)	0.4180(3)	0.4185(3)	0.4188(2)	0.4187(3)	0.4189(3)
$\langle r^{-1}_{e^-x^+}\rangle$	0.3689(4)	0.4806(6)	0.5746(6)	0.6415(5)	0.6826(4)	0.7051(4)	0.7178(4)	0.7240(4)	0.7272(4)	0.7289(4)	0.7295(4)	0.7299(4)
$\langle r^{-1}_{e^+x^+}\rangle$	0.2215(7)	0.2602(9)	0.2924(9)	0.3164(6)	0.3311(5)	0.3388(4)	0.3438(4)	0.3459(4)	0.3470(4)	0.3478(4)	0.3477(4)	0.3479(4)
$\langle\delta(r_{e^-e^-})\rangle$	0.00023(2)	0.00046(4)	0.00073(5)	0.00101(6)	0.00118(7)	0.00134(8)	0.00139(8)	0.00145(8)	0.00147(9)	0.00148(7)	0.00148(8)	0.00146(8)
$\langle\delta(r_{e^-e^+})\rangle$	0.0220(9)	0.0224(9)	0.0230(8)	0.0235(9)	0.0238(9)	0.0240(9)	0.0240(9)	0.0245(9)	0.0243(9)	0.0240(9)	0.0244(9)	0.0242(9)
$\langle\delta(r_{e^-x^+})\rangle$	0.0217(8)	0.051(3)	0.088(5)	0.120(6)	0.143(8)	0.157(9)	0.165(9)	0.169(9)	0.171(9)	0.172(9)	0.172(9)	0.173(9)
$\langle\delta(r_{e^+x^+})\rangle$	0.00023(2)	0.00036(3)	0.00046(4)	0.00055(5)	0.00056(5)	0.00050(4)	0.00050(4)	0.00044(4)	0.00037(3)	0.00034(3)	0.00029(3)	0.00028(3)

TABLE VIII. Expectation values at different nuclear masses for $x^+p^+e^-$: total energy, interparticle distances and their second moments as well as their first inverse moments, and contact densities. Values are given in atomic units, and a 2σ error estimate is shown in the parentheses. For the contact densities, the error estimates also include a contribution resulting from extrapolation to origin. Reading from left to right, the x^+ in the table goes from positron to proton—the mass of the particle increases.

$\log_2(m_x/m_e)$	0.0000	1.0000	2.0000	3.0000	4.0000	5.0000	6.0000	7.0000	8.0000	9.0000	10.0000	10.8425
E	−0.4994(4)	−0.4997(4)	−0.5096(2)	−0.5325(2)	−0.5536(2)	−0.5692(2)	−0.5794(2)	−0.5860(2)	−0.5903(2)	−0.5935(2)	−0.5953(2)	−0.5965(3)
$\langle r_{e^-x^+}\rangle$	144.1(2)	143.9(3)	3.943(9)	2.544(3)	2.121(2)	1.930(2)	1.831(2)	1.775(1)	1.7402(9)	1.7181(9)	1.7046(9)	1.6969(9)
$\langle r_{e^-p^+}\rangle$	1.502(2)	1.501(2)	1.720(3)	1.841(3)	1.850(3)	1.817(2)	1.781(2)	1.753(2)	1.731(1)	1.7139(9)	1.7034(9)	1.6971(9)
$\langle r_{x^+p^+}\rangle$	144.1(2)	143.9(3)	4.189(8)	2.977(3)	2.599(3)	2.396(2)	2.274(2)	2.196(2)	2.143(2)	2.107(2)	2.085(2)	2.072(2)
$\langle r^2_{e^-x^+}\rangle$	22506(54)	22468(76)	21.1(2)	8.44(2)	5.788(9)	4.743(6)	4.235(5)	3.954(5)	3.784(4)	3.677(4)	3.612(4)	3.576(4)
$\langle r^2_{e^-p^+}\rangle$	3.006(6)	3.004(6)	4.07(2)	4.56(2)	4.48(2)	4.239(8)	4.025(7)	3.865(5)	3.747(5)	3.661(4)	3.608(4)	3.576(4)
$\langle r^2_{x^+p^+}\rangle$	22507(54)	22468(76)	21.6(2)	9.91(2)	7.32(2)	6.09(2)	5.403(9)	4.981(8)	4.706(6)	4.523(6)	4.411(6)	4.348(6)
$\langle r^{-1}_{e^-x^+}\rangle$	0.00795(2)	0.00814(9)	0.4084(7)	0.6028(6)	0.7070(5)	0.7646(5)	0.7971(5)	0.8157(5)	0.8270(4)	0.8341(4)	0.8384(4)	0.8410(5)
$\langle r^{-1}_{e^-p^+}\rangle$	0.9989(7)	0.9994(7)	0.9071(7)	0.8426(7)	0.8205(7)	0.8188(6)	0.8227(6)	0.8277(5)	0.8322(5)	0.8366(5)	0.8391(5)	0.8408(5)
$\langle r^{-1}_{x^+p^+}\rangle$	0.00795(2)	0.00812(8)	0.2963(4)	0.3804(3)	0.4202(4)	0.4451(4)	0.4609(4)	0.4713(4)	0.4785(3)	0.4837(3)	0.4868(3)	0.4888(4)
$\langle\delta(r_{e^-x^+})\rangle$	0.000001(2)	0.00001(2)	0.040(3)	0.097(5)	0.140(8)	0.167(9)	0.18(1)	0.19(1)	0.20(2)	0.20(2)	0.20(2)	0.20(2)
$\langle\delta(r_{e^-p^+})\rangle$	0.31(2)	0.31(2)	0.26(2)	0.22(2)	0.21(2)	0.20(2)	0.20(2)	0.20(2)	0.20(2)	0.20(2)	0.20(2)	0.20(2)
$\langle\delta(r_{x^+p^+})\rangle$	0.00(0)	0.00(0)	0.000011(4)	0.0000011(8)	0.00000002(5)	0.00(0)	0.00(0)	0.00(0)	0.00(0)	0.00(0)	0.00(0)	0.00(0)

In Table III, we show the energetics for the system $x^+e^+e_2{}^-$, where m_x is given seven values that can be found in Refs. [22] and [23]. In this case, the mass m_x is also given values smaller than that of an electron. Three of the values reported in Ref. [22] can be considered as highly accurate, since those values agree with our results within our confirmed accuracy, i.e., $0.00081E_h{}^{-1}$. Otherwise, our PIMC results are more accurate and, moreover, our simulations do not indicate the inconsistency found in the values of Ref. [22]. Other observables for this case are given in Table IX.

Due to the finite temperature, the calculated total energy is the one from a minimized NVT ensemble free energy. In this paper, the consequent difference between the zero Kelvin and this total energy is, in general, smaller than the estimated error derived from statistics and from the imaginary-time time step. The only exemptions may occur in the case of $x^+p^+e^-$ for masses $m_x = m_e$ and $m_x = 2m_e$, for which we find noticeable contributions from the entropy; see the first few columns in Table VIII.

The main challenges in the MCDFT are related to the description of light nuclei. Protons in small systems are already treated reasonably well. However, there definitely is room for improvement in that case, and especially in the case of positronic systems. The data presented in Tables I–IX will serve as good reference data in the development and fitting of electron-nuclear energy functionals. It enables one to gradually go towards a proper description of the lightest and most difficult "nucleus," i.e., the positron.

It should be pointed out that proper density-dependent reference data will be essential for the success of MCDFT.

TABLE IX. Expectation values for $x^+e^+e_2{}^-$ using the same values for m_x as in Refs. [22] and [23]. Total energy, interparticle distances and their second moments as well as their first inverse moments, and contact densities are presented. Values are given in atomic units, and a 2σ error estimate is shown in the parentheses. For the contact densities, the error estimates also include a contribution resulting from extrapolation to origin.

m_x/m_e	0.0200	0.1000	0.4690	0.6000	0.6070	0.6560	1.3140
E	−0.2719(2)	−0.3083(2)	−0.4237(2)	−0.4520(2)	−0.4533(2)	−0.4628(2)	−0.5516(2)
$\langle r_{e^-e^-}\rangle$	8.49(4)	8.24(3)	7.05(4)	6.73(4)	6.69(4)	6.62(5)	5.62(4)
$\langle r_{e^-e^+}\rangle$	5.46(2)	5.35(2)	4.90(2)	4.77(2)	4.75(2)	4.73(3)	4.31(2)
$\langle r_{e^-x^+}\rangle$	77.05(6)	17.051(9)	6.19(2)	5.52(2)	5.48(2)	5.31(3)	4.04(2)
$\langle r_{e^+x^+}\rangle$	77.09(6)	17.55(2)	7.58(4)	7.00(4)	6.95(4)	6.81(5)	5.57(4)
$\langle r^2_{e^-e^-}\rangle$	92(2)	85.7(6)	63(1)	57.5(8)	56.8(8)	56(2)	40.0(8)
$\langle r^2_{e^-e^+}\rangle$	47.6(6)	45.2(3)	36.3(5)	33.9(4)	33.6(4)	33.2(6)	26.3(4)
$\langle r^2_{e^-x^+}\rangle$	7709(11)	379.2(5)	52.1(5)	42.3(4)	41.7(4)	39.5(6)	23.9(4)
$\langle r^2_{e^+x^+}\rangle$	7710(11)	394.3(7)	73(1)	61.9(8)	61.0(8)	59(2)	39.3(8)
$\langle r^{-1}_{e^-e^-}\rangle$	0.1564(4)	0.1601(3)	0.1877(6)	0.1968(6)	0.1977(5)	0.2006(7)	0.2368(8)
$\langle r^{-1}_{e^-e^+}\rangle$	0.3404(4)	0.3426(2)	0.3554(4)	0.3590(4)	0.3595(4)	0.3606(4)	0.3748(5)
$\langle r^{-1}_{e^-x^+}\rangle$	0.01934(2)	0.08514(5)	0.2500(3)	0.2866(3)	0.2884(3)	0.3004(4)	0.4141(5)
$\langle r^{-1}_{e^+x^+}\rangle$	0.01925(2)	0.07897(7)	0.1756(5)	0.1904(5)	0.1915(5)	0.1958(6)	0.2378(8)
$\langle\delta(r_{e^-e^-})\rangle$	0.000058(9)	0.000073(8)	0.00012(2)	0.00013(2)	0.00014(2)	0.00015(2)	0.00032(3)
$\langle\delta(r_{e^-e^+})\rangle$	0.020(2)	0.0207(8)	0.0212(8)	0.0215(8)	0.0215(8)	0.0215(8)	0.0222(8)
$\langle\delta(r_{e^-x^+})\rangle$	0.000002(1)	0.00017(1)	0.0060(2)	0.0095(4)	0.0098(4)	0.0110(4)	0.031(2)
$\langle\delta(r_{e^+x^+})\rangle$	0.0000002(3)	0.000008(2)	0.000111(9)	0.00014(2)	0.00013(2)	0.00015(2)	0.00028(3)

Obtaining such results is computationally demanding; however, the authors of this paper are already working on it. For now, the results of this paper give useful complementary information on the energetics of small light-nuclei systems, which can be used in finding better fits for the functionals.

We acknowledge CSC - IT Center for Science Ltd. and TCSC - Tampere Center for Scientific Computing for the allocation of computational resources. For financial support, we thank the Finnish Cultural Foundation and the Physics Department of the University of Illinois at Urbana-Champaign.

[1] T. Kreibich and E. K. U. Gross, Phys. Rev. Lett. **86**, 2984 (2001).
[2] P. Hohenberg and W. Kohn, Phys. Rev. **136**, B864 (1964).
[3] W. Kohn and L. J. Sham, Phys. Rev. **140**, A1133 (1965).
[4] R. van Leeuwen, Phys. Rev. B **69**, 115110 (2004).
[5] R. van Leeuwen, Phys. Rev. B **69**, 199901(E) (2004).
[6] K. Hannewald and P. A. Bobbert, Phys. Rev. B **69**, 075212 (2004).
[7] G. F. Gribakin, J. A. Young, and C. M. Surko, Rev. Mod. Phys. **82**, 2557 (2010).
[8] H. R. J. Walters, Science **330**, 762 (2010).
[9] S. J. Brawley, S. Armitage, J. Beale, D. E. Leslie, A. I. Williams, and G. Laricchia, Science **330**, 789 (2010).
[10] D. M. Ceperley and B. J. Alder, Phys. Rev. Lett. **45**, 566 (1980).
[11] T. Kreibich, R. van Leeuwen, and E. K. U. Gross, Phys. Rev. A **78**, 022501 (2008).
[12] A. Chakraborty, M. V. Pak, and S. Hammes-Schiffer, Phys. Rev. Lett. **101**, 153001 (2008).
[13] D. M. Ceperley, Rev. Mod. Phys. **67**, 279 (1995).
[14] I. Kylänpää and T. T. Rantala, J. Chem. Phys. **135**, 104310 (2011).
[15] R. P. Feynman, *Statistical Mechanics* (Perseus Books, Reading, MA, 1998).
[16] R. G. Storer, J. Math. Phys. **9**, 964 (1968).
[17] N. Metropolis, A. W. Rosenbluth, M. N. Rosenbluth, A. H. Teller, and E. Teller, J. Chem. Phys. **21**, 1087 (1953).
[18] C. Chakravarty, M. C. Gordillo, and D. M. Ceperley, J. Chem. Phys. **109**, 2123 (1998).
[19] M. F. Herman, E. J. Bruskin, and B. J. Berne, J. Chem. Phys. **76**, 5150 (1982).
[20] J. Usukura and Y. Suzuki, Phys. Rev. A **66**, 010502 (2002).
[21] J. Mitroy and M. W. J. Bromley, Phys. Rev. A **73**, 052712 (2006).
[22] J. Mitroy and S. A. Novikov, Phys. Rev. A **70**, 032511 (2004).
[23] M. W. J. Bromley and J. Mitroy, Phys. Rev. A **66**, 062504 (2002).
[24] G. W. F. Drake, M. M. Cassar, and R. A. Nistor, Phys. Rev. A **65**, 054501 (2002).
[25] A. M. Frolov, Phys. Rev. A **58**, 4479 (1998).
[26] D. M. Bishop and L. M. Cheung, Phys. Rev. A **16**, 640 (1977).
[27] S. Bubin and L. Adamowicz, Phys. Rev. A **74**, 052502 (2006).
[28] M. Stanke, D. Kedziera, S. Bubin, M. Molski, and L. Adamowicz, J. Chem. Phys. **128**, 114313 (2008).